International Journal of Applied Engineering Research ISSN 0973-4562 Volume 12, Number 16 (2017) pp. 6029-6036

Analysis of Cast in Place Piles Using Finite Elements Method

Riyadh Razzaq Salim[1]
Assistant Research, College of Engineering, University of Basrah, Basrah, Iraq.

Dr. Oday Adnan Abdulrazzaq[2]
Lecturer, College of Engineering, University of Basrah, Basrah, Iraq.

Orcid ID: 0000-0001-7619-9341

Abstract

This thesis aims to use finite elements method to investigate the response of a single cast in place pile, embedded in multi-layers soil at the Project of AL-Nasiriya New Oil Depot, under the effect of vertical static load. ABAQUS 6.14.3 program was used in this analysis. The piles and the surrounding soil were modeled using three-dimensional brick linear elements. Several cases of pile diameters (0.6m, 0.8m, 1.0m, and 1.2m) and lengths (16m, 18m, 20m, and 22m) were adopted to study their effects on the pile capacity. The results of the analysis were represented by failure loads and ultimate loads in addition to the settlement values and compared with the values computed using the analytical or empirical methods.

Keywords: Cast in place piles, Finite element analysis, pile load capacity, Soil pile interaction.

INTRODUCTION

Piles are long structural members that have the function of transmit loads from the superstructure through weak strata or through water, onto stiffer or more compact and less compressible soils or onto rock [1]. Piles are generally used when soil conditions are not suited for the use of shallow foundations. Piles resist applied loads through side friction (skin friction) and end bearing. Friction piles resist a significant portion of their loads by the interface friction developed between their surface and the surrounding soils. On the other hand, end-bearing piles rely on the bearing capacity of the soil underlying their bases. Usually, end-bearing piles are used to transfer most of their loads to a stronger stratum that exists at a reasonable depth [2].

Piles that penetrate a relatively soft layer of soil to found on a firmer stratum are referred to as ‘end-bearing’ piles and will derive most of their capacity from the base capacity. Where no particularly firm stratum is available to found the piles on, the piles are known as ‘friction’ or ‘floating’ piles [3].

The core of problems in the design of the piles and foundations are settlement and bearing capacity of single pile. It is virally important for the design of whole piles and foundation to compute and analysis them accurately. At the present, there are three mainly methods to solve this problem which are analytical methods, pile load test and numerical methods [4].

Ottaviani and Marchetti [5] made a comparison between experimental results that obtained from loading tests on an instrumented pile, with the results obtained from a non-linear finite element analysis based on the geometry and the geotechnical parameters determined by standard in situ and laboratory investigations. The pile was of bored type with (0.6m) diameter and (23.5m) length, embedded in multi-layer soil. it was used 2D axisymmetric model with 396 elements and 444 nodes for the total model. They found a good agreement between the experimental results with that resulted from finite element method.

Chin et al. [6] used the numerical analysis to simulate vertical loaded piles and pile groups. The results were compared with the existed published solutions for the cases of piles in homogeneous soil, end-bearing piles on stiffer layer, and piles in Gibson soil. They obtained there was a good agreement between the numerical solutions and the published solutions.

F. Kirzhner [7] analyzed a single pile of length (20m) and diameter (0.9m) under vertical load to estimate its ultimate load capacity. Also he studied the mechanism of shaft friction. He used FLAC Program for the finite element analysis to estimate the ultimate load capacity for the pile. He discussed the bearing capacity of the piles, embedded in sandy soil, under the effect of different shapes of the pile (cylinder, conical, combiner cylinder and combiner inverse cylinder) and estimated the displacements for these types of piles. Mohr- coulomb theory used to describe the soil behavior, while the concrete material of the pile was assumed to be linearly elastic. The results of numerical method were compared with the field loading test results. It was found that, for the same volume of pile, the larger base area caused a reducing in the settlement values and accordingly the bearing capacity of the pile increased. Also, the cylindrical pile was better than the conical, because of its resistance against penetration was better. He also found that the inverse

combined cylinder was better than the regular, because it has a wide base.

B. P. Naveen et al. [8] used finite elements method to simulate field vertical load test on a single bored pile of (1.2m) diameter and (15m) length embedded in multi layers soil using PLAXIS 2D. The soil was modeled as elastic-plastic based on the Mohr- coulomb theory, while pile material was assumed as a linear-elastic. Interface elements was used to model the interface between the pile and soil. A reasonable agreement was obtained from the a comparison between the load-settlement curve obtained from field test with that resulted from the finite element analysis. Also, it was concluded that Mohr-coulomb model with medium mesh is optimum for simulating the settlement of vertical loaded pile in residual soils.

Kasimierz [9] analyzed a soil-pile system using ABAQUS software. The ultimate load capacity and settlement of pile resulted from the finite element analysis were compare with the results of static load test and engineering calculations according to Eurocode7 and Polish standard Code. The pile material was assumed as linear elastic and the soil was modeled as elastic-plastic with constitutive models of Mohr-coulomb and Drucker- Prager. It was used two dimensions (2D) with axisymmetric model for pile-soil system. Two models were used to simulate the interaction between the pile and the surrounding soil; the first one was a simple coulomb friction model, while in the second model, it was assumed a contact condition with constrained relative motion between the pile and the surrounding soil "tied". For the loading part, the finite element analysis showed a quite good agreement with the results of the field test. A significant difference for the unloading case was observed. It was found that the "elastic slip" in comparison with contact formulation "tied" had some impact on the results. The constitutive models that used to describe the soil material gave different results for the pile bearing capacity. The difference were explained due to the lack of the detailed data characterizing soil layer.

This study aims to use finite elements method to analyze and predicting the load capacity for a single cast in place pile subjected to vertical load at the site project of "AlNasiriya New Oil Depot" which located at Thi-Qar Governorate in the south of Iraq, as shown Fig. (1). ABAQUS 6.14.3software was used to implement this analysis for two cases; in the first case, four values for pile diameter (0.6m, 0.8m, 1.0m, and 1.2m) with constant length of (18m) were assumed, while in the second case, four values for pile length (16m, 18m, 20m, and 22m) with constant diameter of (0.8m) were assumed.

Figure 1: Al Nasiriya New Oil Depot site location.

2. Static pile capacity

All static compression pile capacities can be computed by the following equation[10];

$$P_u = P_b + \Sigma P_s \quad \text{..... (1)}$$

Where;

P_b: Ultimate point capacity (kN)

P_s: Skin resistance (kN)

Hansen's equation could be used to calculate ultimate point capacity for the pile, as follows;

$$P_b = A_b(CN_c d_c S_c + \eta q' N_{q'} d_{q'} S_{q'} + \frac{1}{2}\gamma' D_p N_\gamma S_\gamma) \quad \text{..... (2)}$$

Where

A_b: Area of pile point effective in bearing.

C: Cohesion of soil beneath pile point.

D_p: Width of pile.

N_c, $N_{q'}$, N_γ: Non-dimensional parameters of bearing capacity and are dependent on the angle of internal friction of soil as shown in table below:

$$d_c = 1+0.4tan^{-1}(\frac{D_p}{L}) \quad \text{..... (3)}$$

L: length of pile.

$$d_{q'} = 1+2\tan\phi\,(1-\sin\phi)^2 tan^{-1}(\frac{D_p}{L}) \quad \text{..... (4)}$$

q': over-burden pressure at end pile

$\eta = 1$

To calculate skin friction resistance, it could be used equations of α method which proposed by Tomlinson [11], as below;

$$P_s = (\alpha\, C)\, A_s + (q' k \tan\delta)\, A_s \quad \text{..... (5)}$$

As: Effective pile surface area.

For concrete bored pile, α = 0.45, δ = 0.75Ø, k = (1 for loose soils or 2 for dense soils).

PERMISSIBLE SETTLEMENT FOR PILE

To calculated the permissible settlements of the piles at working load, an empirical equation shown below [12];

$$S_t = \frac{D_p}{100} + \frac{PL}{A_b E} \quad \text{..... (6)}$$

S_t: Settlement of pile head

P: The applied pile load

E: Modulus of elasticity of the pile material

FINITE ELEMENTS MODELING

The finite elements method combines, in an elegant way, the best features of many approximate methods. The technique is amenable to systematic computer programming and offers scope for application to a wide range of problems. The basic concept is that a body or structure may be divided into smaller elements of finite dimensions called "finite elements". The original body or the structure is then considered as an assemblage of these elements connected at a finite number of joints called "nodes" or "nodal points". The properties of the elements are formulated and combined to obtain the solution for the entire body or structure. One of the finite element commercial codes widely used in the research and designing process is ABAQUS which is a finite element analysis software program.

In this study, it was used three-dimensional finite elements for analyzing the studied models. Since the soil boundaries for a single pile have to be taken at distance range of (6-18) times of pile diameter or width below from the pile tip [13]. In this study, it is assumed that the soil mas extends to depth of (10D), while its diameter equals to (30D), where (D) is the diameter of the pile.

Since the identification of the line of symmetry in loading, geometry, and material conditions in the problem allows to modeler for reducing the size of the model [14]. For circular pile under pure axial load, one-half of problem size was used to reduce time of computation. The displacement values at the outer edges of the model were assumed equal to zero, as shown in Fig. (2).

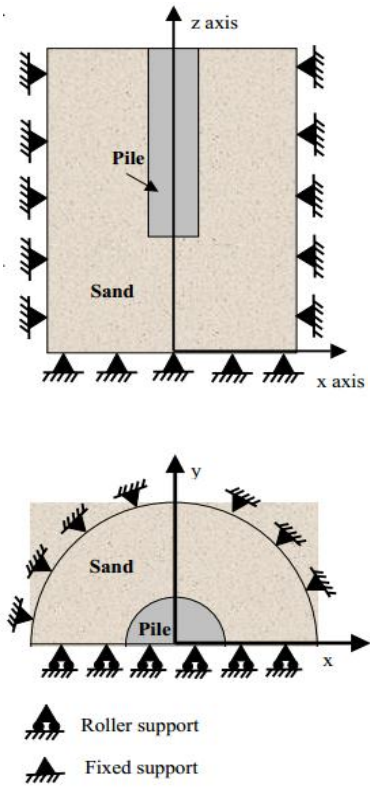

Figure 2: Boundary conditions in the symmetry plan and outer edge of the model.

The 8-nodes linear element (C3D8R) is used for discretizing both pile and soil for all models as shown in Fig. (3). The interaction between the pile and the surrounding soil was simulated by penalty method. This type of interface is used so that permits some relative motion between surfaces (elastic slip). The master-slave concept, shown in Fig. (4), was used to define the contact surfaces. The contact elements is paced along the shaft and base of the pile. The normal stress is transmitted in the normal direction of the master surface, while the shear stress is transmitted tangentially according to simple coulomb friction model with coefficient of friction equal to tan δ, δ = (2/3)Ø [15]. In this study, the pile was defined as a master and the soil as a slave.

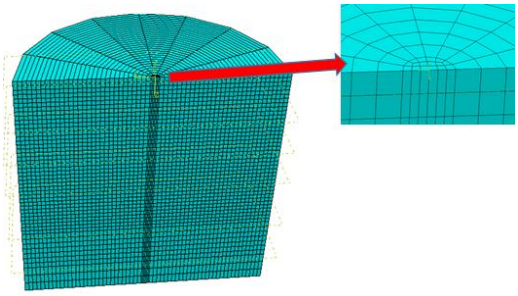

Figure 3: Typical pile-soil mesh.

Materials behavior of the concrete and the rebar reinforcements for the piles were assumed as linearly elastic,

as listed in Table (1). While the behavior of the material for the surrounding soil was assumed as elastic-plastic based on the Mohr-coulomb model. Table (2) lists the properties of the soil profile at the project of AL-Nasiriya New Oil Depot.

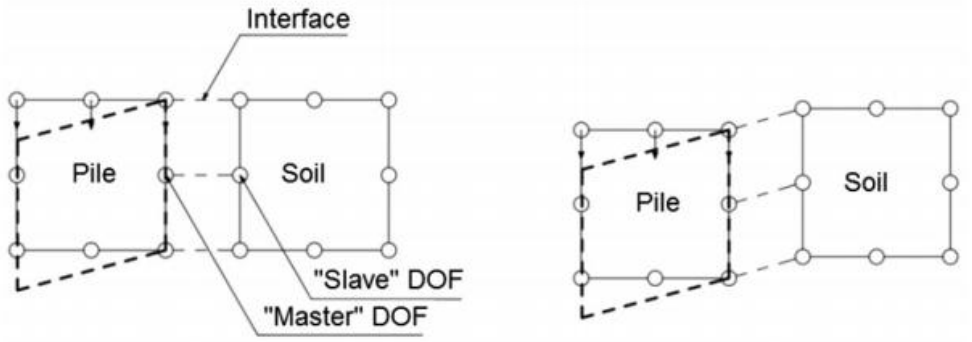

Figure 4: Master-Slave concept. [16]

Table 1: Properties of the pile materials.

Parameter	Symbol	Unit	Concrete	Rebar
Unite weight	γ	kN/m^3	24	78
Compressive strength	f_c'	kPa	37500	------
Young's modulus	E	MPa	28780	200000
Poisson's ratio	υ	------	0.2	0.3
Yield stress	f_y	MPa	------	625

Table 2: Soil properties at the site of AL-Nasiriya New Oil Depot. [17]

Layer	Properties					
	Unite weight (γ) (kN/m^3)	Young's modulus (E) (MPa)	Poisson's ratio (υ)	Cohesion intercept (c) (kPa)	Friction angle ($Ø^\circ$)	Dilation angle (ψ°)
Clay (0-3.5m)	16.35	50	0.35	321	21	0
Clay (3.5-6m)	19.60	35	0.35	74	11	0
Clay (6-15m)	9.37	35	0.35	70	11	0
Sand (15-23m)	10.19	55	0.30	0.1	36	6
Sand (23-50m)	12.23	80	0.30	0.1	40	10

APPLICATIONS, RESULTS AND DISCUSSION

Influence of piles diameter

Four models of different diameters for the pile were studied to determine their effects on the pile capacity with assuming a constant pile length of (18m), as shown in Table (3).

Table 3: Models of studied piles with different diameters.

Model	Pile's diameter (m)
1	0.6
2	0.8
3	1.0
4	1.2

Pile load was applied in increments of (220kN) for each 2.5 mins. This loading process stopped when the settlement of top pile reached to 15% from diameter of pile base [18].

The numerical results of the settlements, at the top face of the piles, under the effect of the applied loads are shown in the Fig. (5). It can be noted that load-settlement curves for the four models of pile diameters have the same behavior. It was noted that the rate of settlements rapidly increase after load values of (990kN, 990kN, 1980kN and 1980kN) for models (1, 2, 3, and 4, respectively), where the settlement values increase with the increasing of the applied load until failure corresponding to settlement values equal to (15%) from the pile diameters. After removing the applied load, the residual settlements are (52mm, 70mm, 77mm, and 86mm) for the models (1, 2, 3, and 4, respectively).

Table (4) lists the maximum values of axial stresses and failure loads which resulted from the finite elements analysis. It was shown that maximum values of the axial stresses computed at the top faces of piles decreased about 7.6%, 12.6%, and 38.8% for models (2, 3, and 4, respectively) compared to that of model (1). Also, it can be noted that the designed compressive strength (37500kPa) for the concrete material of the piles was not exceeded in the four models of the studied piles. Failure loads for the piles in models (2, 3, and 4) increased about (58%, 156.5%, and 253.2%, respectively) compared to the failure load for model (1). This increasing in the computed failure loads and the decreasing in the maximum axial stresses on the top faces of the piles could be illustrated to the increasing in the end bearing resistance with increasing pile diameters.

The values of estimated ultimate loads and the computed analytical loads for the studied models of the piles are listed in Table (4). Davisson's method [19] was used to estimate the ultimate pile capacities from Fig. (5). The ultimate loads for the piles in models (2, 3, and 4) increased about (46.4%, 128.9%, and 244.4%, respectively) compared to model (1). From the comparison between the analytical ultimate load, which computed using Eq. (1), with the estimated ultimate load, it was found that the results of the estimated ultimate loads were less about (9.6%, 18.7%, 14.0%, and 12.4%) for models (1, 2, 3, and 4, respectively).

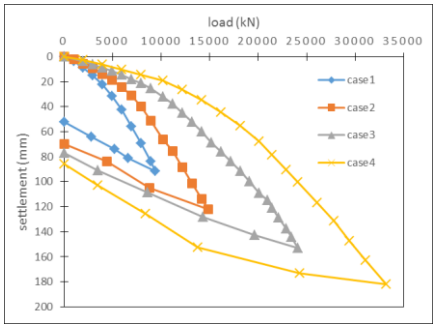

Figure 5: Load-settlement curves for different values of pile diameters.

Table 4: Results of the maximum axial stresses, failure loads, estimated ultimate loads, and analytical ultimate loads for different values of pile diameters.

Model	Maximum axial stress at top face of the pile (kPa)	Failure load (kN)	Estimated ultimate load (kN)	Analytical ultimate load (kN)
1	30452.8	9400	2970	3284
2	28143.6	14850	4350	5352
3	26605.8	24110	6800	7912
4	18630.3	33200	10230	11686

Table (5) lists the results of the finite elements analysis for maximum settlement values at top and bottom faces of the studied models of the piles. It shows that the settlement values computed at top faces are larger compared to that computed at the bottom faces about (23.8%, 14.2%, 10.7%, and 7.8%) for models (1, 2, 3, and 4, respectively). This differences in values of the settlement between top and bottom faces of the piles could be illustrated due to the axial deformation of pile.

Table 5: Settlement values at top and bottom faces of studied models for different values of pile diameters.

Model	Pile's settlement at top face (mm)	Pile's settlement at bottom face (mm)
1	91.6	74.0
2	122.2	107.0
3	153.1	138.3
4	182.2	169.0

Table (6) lists the permissible settlements values, computed using the Eq. (6), and the allowable settlement values which found from Fig. (5). The two values of settlements are corresponding to the allowable load values which computed by dividing the estimated ultimate loads by a safety factor of (2). It can be noted that the permissible settlements are greater than allowable settlements about (48.5%, 75%, 76 % and 82.6%) for models (1, 2, 3, and 4, respectively).

Table 6: Permissible and allowable settlements for different values of pile diameters.

Model	Allowable load (kN)	Permissible settlement (mm)	Allowable settlement (mm)
1	1485	9.28	6.25
2	2175	10.71	6.12
3	3400	12.71	7.22
4	5115	14.83	8.12

Influence of piles length

To study the effect of the length on piles capacity, it was used four different values for pile lengths with constant diameter of (0.8m), as listed in Table (7).

Table 7: Models of studied piles with different lengths.

Model	Pile's length (m)
1	16
2	18
3	20
4	22

The piles were assumed to be loaded in the same manner that mentioned previously until the failure. The results of deflection under the effect of applied loads are shown in Fig. (6). As mentioned in the previous section, load-settlement curves for the four models of pile lengths have the same behavior and the rate of settlement values rapidly increases after load values of (990kN, 990kN, 1980kN and 1980kN) for models (1, 2, 3, and 4, respectively) until reaching to the failure load, which corresponding to settlement value equal to (15%) from the pile diameters. As the pile reaches to failure, the unloading stage start and the load decrease to zero value. The residual settlements, after removing the load, are (83.6mm, 70mm, 66.8mm, and 73mm) for the models (1, 2, 3, and 4, respectively).

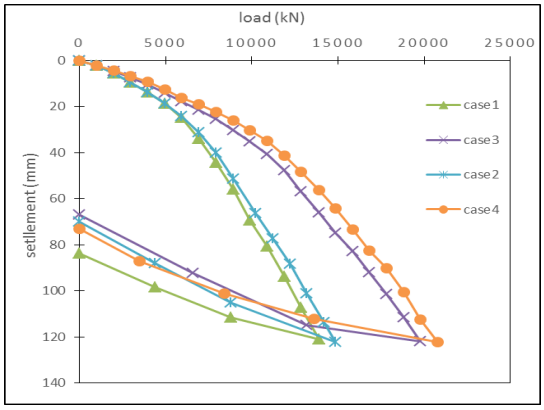

Figure 6: Load-settlement curves for different values of pile lengths.

Table (8) lists the results of finite elements analysis for maximum axial stresses computed at the top faces of the piles and the failure loads for the studied models. The maximum axial stresses at the top faces of the piles increased about (2.1%, 28.2%, and 31.5%) for models (2, 3, and 4, respectively) compared to that computed for model (1). It could be noted that the designed compressive strength (37500kPa) for the concrete material of the piles was not exceeded in the four cases of the pile lengths. The failure loads for the studied models in models (2, 3, and 4) increased about (6.9%, 42.5%, and 49.6%, respectively) compared to the failure load of model (1). This increasing in the computed failure loads and in the maximum axial stresses at the top faces of the piles could be illustrated to the increasing in the skin resistance with increasing pile lengths in the sandy layer.

As in the previous section, Davisson's method was used to estimate the ultimate load capacity for the studied models of the piles from Fig. (6), as listed in Table (8). It could be noted that the estimated ultimate load capacities for models (2, 3, and 4) increased about (6.1%, 48.8%, and 84.1%, respectively) compared to model (1). Also, this table lists the analytical ultimate loads which computed using Eq. (1). The analytical ultimate loads for models (1, 2, and 3) are greater than the estimated ultimate loads about (13.1%, 23%, and 0.03%, respectively), but the analytical load capacity was (8.8%) lesser in the case of model (4).

Table 8: Results of the maximum axial stresses, failure loads, estimated ultimate loads, and analytical ultimate loads for different values of pile lengths.

Model	Maximum axial stress at top face of the pile (kPa)	Failure load (kN)	Estimated ultimate load (kN)	Analytical ultimate load (kN)
1	27558.4	13890	4100	4636
2	28143.6	14850	4350	5352
3	35334.4	19800	6100	6102
4	36238.9	20790	7550	6888

It could be noted from Table (9), that the computed settlement values at top faces of the studied models of the piles are (11.5%, 14.2%, 25%, and 27.4%) larger compared to that computed at bottom faces for models (1, 2, 3, and 4, respectively). As mentioned previously, this differences in the computed settlement between top and bottom faces of the studied models could be illustrated due to the axial deformation of the piles.

Table 9: Settlement values at top and bottom faces of studied models for different values of pile lengths.

Model	Pile's settlement at top face (mm)	Pile's settlement at bottom face (mm)
1	121.0	108.5
2	122.2	107.0
3	121.8	97.4
4	122.2	95.9

Corresponding to the allowable load values which computed by dividing the estimated ultimate loads by a safety factor of (2), Table (10) lists the permissible settlements values which calculated using Eq. (6) and the allowable settlement values which found from Fig. (6). It could be noted that the permissible settlements are (76.9%, 75%, 60.8% and 54.4%) greater than allowable settlements for models (1, 2, 3, and 4, respectively).

Table 10: Permissible and allowable settlements for different values of pile lengths.

Model	Allowable load (kN)	Permissible settlement (mm)	Allowable settlement (mm)
1	2050	10.26	5.80
2	2175	10.71	6.12
3	3050	12.22	7.60
4	3775	13.74	8.90

CONCLUSIONS

From the results of the finite element analysis for the studied models of piles at the site of project "AL-Nasiriya New Oil Depot Site", the conclusions can be summarized as follows;

1- For the piles of (18m) length, increasing of pile's diameter from (0.6m) to (0.8m, 1.0m, and 1.2m) caused an increasing of the estimated ultimate load capacity, which computed using Davisson's method, for the piles about (46.4%, 128.9%, and 244.4%, respectively).

2- For the piles of (18m) length, increasing of pile's diameter from (0.6m) to (0.8m, 1.0m, and 1.2m) caused a decreasing in the maximum values of the axial stresses computed at the top faces of piles about (7.6%, 12.6%, and 38.8%, respectively).

3- For the piles of (0.8m) diameter, the estimated ultimate load capacity for the pile increased to about (6.1%, 48.8% and 84.1%) with increasing the pile lengths from (16m) to (18m, 20m, and 22m, respectively).

4- For the piles of (0.8m) diameter, the computed maximum axial stresses at the top faces of the modeled piles increased about (2.1%, 28.2%, and 31.5%) with increasing the pile lengths from (16) to (18m, 20m, and 22m, respectively).

5- The designed compressive strength (37500kPa) for the concrete material of the piles was not exceeded in all studied models.

REFERENCES

[1] Tomlinson, M. and Woodward, J. ,2008, "Pile Design and Construction Practice", Talyor and Francis Group, London and New York, Fifth Edition.

[2] Austin Weltman, Mark Randolph, Keith Elson, and Ken Fleming, 2008, "Piling Engineering". CRC press.

[3] Prakash, Shamsher, and Hari D. Sharma. , 1989, "Pile Foundations in Engineering Practice". John Wiley and Sons.

[4] Hua Bing and Chen Hao, 2010, "Nonlinear FEM Analysis of Bearing Capacity and Sedimentation of Single Pile in Multi-layered Soils", Proceedings of the International Conference on Computing in Civil and Building Engineering.

[5] Mario, O, and Marchetti, S., 1979, "Observed and Predicted Test Pile Behaviour", International Journal for Numerical and Analytical Methods in Geomechanics 3.2, PP. 131-143.

[6] Chin, J. T., Chow, Y. K., and Poulos, H. G., 1990, "Numerical Analysis of Axially Loaded Vertical Piles and Pile Groups", Computers and Geotechnics, 9(4), PP. 273-290.

[7] Kirzhner, F. and Rosenhouse, G., 2001, "Analysis of the Ultimate Bearing Capacity of a Single Pile in Granular Soils", WIT Transactions on Engineering Sciences.

[8] Naveen, B. P., Sitharam, T. G. and Vishruth, S., 2011, "Numerical Simulation of Vertically Loaded Piles", Young, 21(22.00).

[9] Józefiak, K., Zbiciak, A., Maślakowski, M. and Piotrowski, T., 2015. "Numerical Modelling and Bearing Capacity Analysis of Pile Foundation". Procedia Engineering, 111, PP. 356-363.

[10] Joseph E. Bowles, 1997, "Foundation Analysis and Design", McGraw Hill Companies, Inc.

[11] Shmasher Prakash and Hari D. Sharma, 1989, "Pile Foundation in Engineering Practice", John Wiley and Sons, Inc.

[12] Vesic, A.S., 1970, "Load Transfer in Pile-Soil Systems", Proceeding Conference on Design Installation of Pile Foundations, Lehigh University, Bethlehem, 47-73.

[13] Sarmad, A. 2013, "Finite Element Analysis of Pile Groups Subjected to Lateral Loads", Ph. D. Thesis, University of Basrah, College of Engineering, Civil Engineering Department.

[14] Said, I. D., De Gennaro, V., and Frank, R., 2009, "Axisymmetric Finite Element Analysis of Pile

Loading Tests", Computers and Geotechnics, 36(1), PP. 6-19.

[15] Mohammad, H., Hajitaheri, M., and Hassanlourad, M., 2015, "Numerical Modeling of the Negative Skin Friction on Single Vertical and Batter Pile", Acta Geotechnica Slovenica 12.2, PP. 46-55.

[16] Wrana, B., Kalisz, W. and Wawrzonek, M., 2013, "Nonlinear Analysis of Pile Displacement Using the Finite Element Method", Czasopismo Techniczne. Budownictwo, P. 110.

[17] CPP, 2015, "Geotechnical Survey and Soil Investigation Report for New Nassiriya Depot (Crude Oil Storage Tank Area)".

[18] American Society for Testing and Materials (ASTM), 2007, "Standard Test Method for Piles Under Static Axial Compression Load", D1143/D1143M.

[19] Davisson, M. T., 1972, "High Capacity Piles", Proceedings, Lecture Series Innovations in Foundation Construction, ASCE, Illinois section, Chicago, P. 52.